TRANSMISSION OF ENERGY ALONG ACOUSTIC WAVEGUIDES FOR MICROACTUATION

James Friend[†,*]**, Kentaro Nakamura**[†]**, and Sadayuki Ueha**[†]
[†]Precision and Intelligence Laboratory, Tokyo Institute of Technology, Yokohama, Japan
[*]e-mail: jamesfriend@ieee.org

Abstract

Using a 3 x 3 x 5 mm torsional transducer attached to a 0.3-mm diameter stainless steel wire, coupled torsional-axial-flexural vibration is transmitted along the length of the wire, over 30 cm. Standing wave ratios of 7.5, 4, and 1.5 were measured using a free waveguide tip, tip with rotor, and damped tip. The few torsional resonances of the transducer were found to be greatly increased in number by the waveguide, and rotors, with a contact radius of 300 μm, were found to rotate for most of these resonances at up to 11,500 rpm and 2.5 μN-m.

Introduction

This paper describes the use of acoustic waveguides—essentially wires transmitting vibration along their length—for microactuators. Driven by a piezoelectric microtransducer, the concept permits remote actuation via the flexible waveguide, permitting actuation for example, in harsh environments, in the human body during surgery, or upon weight-critical components where the mass of a motor is unacceptable, such as on the end effector of a robotic arm. Though other forms of remote actuation exist, including hydraulics, belt/chain drives, and cable push/pull or rotation systems, each have limitations, particularly in their response time and their ability to be scaled down to millimeter sizes and beyond.

In work by Ueha, et al. [1], large acoustic waveguides have been studied for lithotriptors, where high power axial vibrations were generated by a Langevin transducer and transmitted along the waveguide to its end. Unfortunately, bending the waveguide causes flexural vibration to appear. Carotenuto, et al. [2], more recently studied the generation of flexural vibrations along a 0.8-mm waveguide by an attached 32-mm disk to form a piezoelectric motor. They used a traveling wave generated by the combination of dual signal drives in the disk to generate a traveling flexural wave along the waveguide. The effect of curvature was considered in their work; they found that if the curvature was greater than the wavelength, the effect of curvature was nearly negligible.

In this paper, a much smaller actuator is used, with a ϕ0.3-mm diameter, 30-cm long stainless steel waveguide, swaged into the tip of a 3×4×8 mm torsional transducer. The transducer is driven from 150–300 kHz

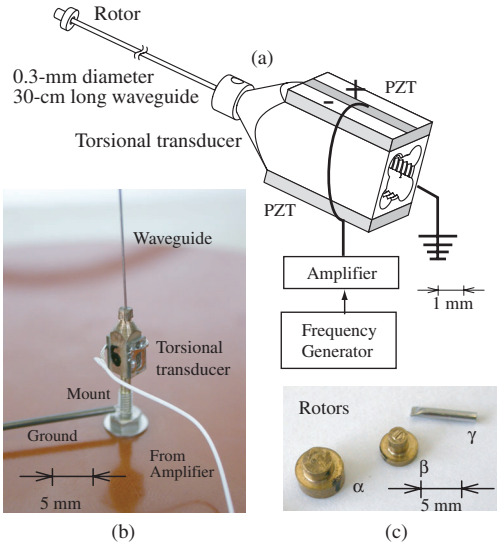

Figure 1: Configuration of the waveguide actuator (a), photograph of the mounted transducer and attached waveguide (b), and (c) rotors α, β, γ.

with a single sinusoidal input signal; evidence of the transducer's torsional vibration is provided, followed by the measurement results of the waveguide's vibration along its length and at its tip. The effect of leaving the tip free, using a rotor, or clamping a damping material of the tip is presented. Finally, the performance of the system as an actuator is shown while varying the applied frequency, waveguide curvature, and rotor configuration.

Experiment

The general arrangement of the actuator is shown in Fig. 1. The transducer uses a pair of piezoelectric elements on either side of a phosphor bronze horn, and generates torsional vibration. Each element bends in-plane due to the opposite through-thickness poling on either side of the element as indicated with a "+" and "−" in the figure, causing twisting of the structure described by Friend, et al. [3].

The waveguide is swaged in a 1-mm deep hole in the tip of the transducer. Though the waveguide is shown straight in the figure, it is very flexible. For the purposes of this study, three rotors were used; their properties are listed in Table 1. The moment of inertia is about the axis of rotation. The rotor was set atop the waveguide using gravity to supply the preload for this study. Magnetic or mechanical attachment would be more practical

Table 1: Rotor Properties

Rotor	Material	Mass (g)	Mom. of Inertia (g-mm^2)
α	PB‡	0.33	1.75
β	PB	0.12	0.26
γ	SS★	0.040	0.16

‡PB = phosphor bronze, ★SS = stainless steel 304

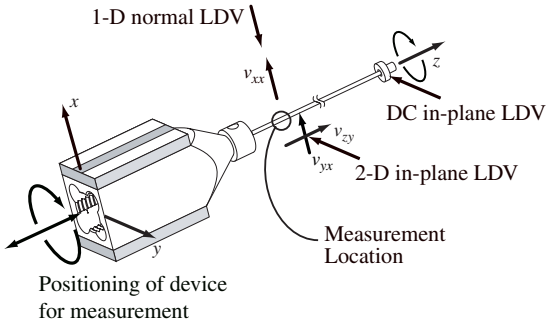

Figure 2: Vibration and rotor velocity measurement configuration. The 2-D in-plane LDV and 1-D normal LDV measure the vibration, while the DC in-plane LDV measures the rotation of the rotor.

in an actual application, but with this configuration altering the waveguide or replacing the rotor was quick and straightforward.

A frequency generator, driving a high-frequency amplifier, was used to generate the input signal, and a series of laser Doppler vibrometers (LDV), including a 2-D in-plane LDV, a DC normal LDV, and a high-frequency normal LDV, as shown in Fig. 2 were used to measure the vibration velocity of the transducer tip, the waveguide, and the rotation speed of the rotor. Knowing the rotor speed with respect to time from start to peak speed, the torque versus speed of the actuator may be determined using a technique described by Nakamura, et al. [4]. It is important to note the rotation of the rotor closely matched the fitting technique described in Nakamura's paper. The entire actuator can be repositioned to change the measurement location.

Results

The vibration velocity of the transducer tip with respect to frequency is provided in Fig. 3(b), with an explanation of the orientation of each velocity in Fig. 3(b). To confirm the orientation of the tip's vibration (axial, flexural in x-direction, flexural in y-direction, or torsional), the vibration velocity was measured in six directions as indicated. The flexural vibrations, indicated by v_{xx} and v_{yy} were generally small, as were the axial vibrations v_{zx} and v_{yz}. However, v_{xy} and v_{yx} were not small, and were essentially the same (except from 240

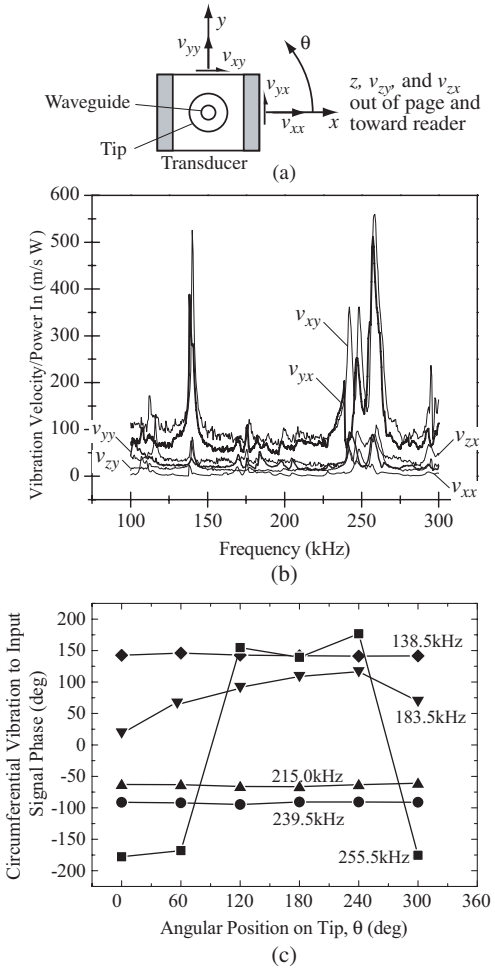

Figure 3: The vibration velocities of the transducer tip per unit power input into the transducer versus frequency.

to 255 kHz where some flexural vibration was generated). Since these velocities were not small, while the flexural vibration *was* small, torsional vibration can be shown to be generated at the transducer's tip. There are torsional resonance frequencies at several frequencies from 100 to 300 kHz. The 2-D in-plane LDV has a smaller signal-to-noise ratio, causing the noise floor for v_{xy} and v_{yx} to be higher in the figure. To *make certain* that the vibrations were indeed torsional, the vibration velocity in the circumferential direction was measured around the tip, as shown in Fig. 3(c). If the vibration is indeed torsional, the phase of the circumferential vibration will be nearly the same all around the tip. Note that it is at 138.5, 183.5, 215.0, and 239.5 kHz. At 255.5 kHz, where v_{xx} is not negligible, there is a complete change in phase from -180 to 180 deg., indicating the presence of flexure in the vibration mode.

As the vibration is conducted along the waveguide, the conditions at the free end determine the type of vibration generated. Fig. 4 illustrates the effect of three different end conditions on the flexural vibration (v_{xx})

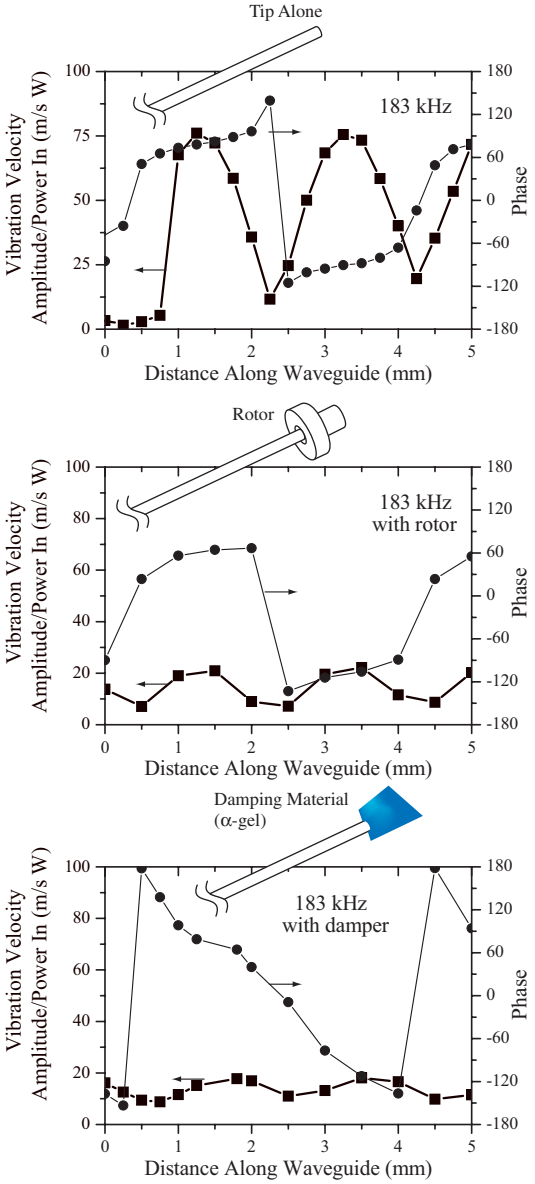

Figure 4: The vibration along 5 mm of the waveguide nearest the transducer for free, with rotor, and damped end conditions, all at 183.5 kHz.

of the first five millimeters of the waveguide: free, with a rotor on the tip, and with α-gel damping material firmly clamped to the tip. The standing wave motion is present not only for flexible vibration, but also for torsional and axial vibration, each having different wavelengths. The standing wave ratio (ratio of maximum to minimum vibration velocity amplitude) and amplitude of the v_{xx}, v_{yx}, and v_{zx} vibrations are provided in Table 2. With the tip free, a standing wave is present in the waveguide, indicating reflection of the acoustic energy from the waveguide tip back toward the transducer. Once the rotor is placed upon the tip, the vibration magnitude to input power ratio is greatly reduced, and much of the energy is conducted to the rotation of the rotor, creating a travelling wave. With a damped end, the vibration is reduced further, and the travelling

Table 2: Amplitude and Standing Wave Ratio of Waveguide Vibration at 183.5 kHz

	v_{xx}		v_{yx}		v_{zx}	
	A[††]	SWR[♯]	A	SWR	A	SWR
Tip Alone	750	7.5	900	9.2	650	7.9
Rotor	20	4.0	40	4.5	20	2.5
Damping	650	1.5	20	2.5	20	1.2

[††]A = amplitude of vib. vel./unit power input (m/s·W),
[♯]SWR = standing wave ratio

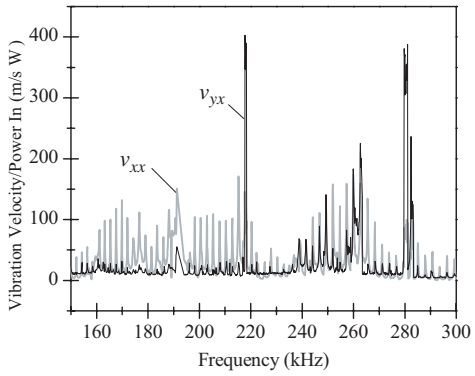

Figure 5: The vibration velocities of the waveguide tip per unit power input into the transducer versus frequency.

wave is even more prominent.

As Fig. 5 shows, the waveguide discretizes the output of the transducer, and causes the generation of flexural motion not present in the transducer. Both results are not surprising since it is very easy to excite flexural vibration in the waveguide. Comparing the magnitude of vibration in Figs. 3(b) and 5, the attenuation of the waveguide does not appear to be significant under these conditions. The presence of a strong standing wave as described before would tend to confirm this result.

For almost every resonance peak in Fig. 5, it is possible to rotate a rotor placed on the end of the waveguide. Rotation in either direction is possible depending on the chosen resonance frequency, as illustrated in Figs.6 and 7. Though not shown here, rotation at up to 551 kHz was obtained. The actuator gives extremely high rotation speeds with a concomitant low torque. Since the contact radius is 300 μm, this result is to be expected. The response time of the γ rotor (from zero to maximum rotation speed) was about 15 ms in either direction.

Finally, the effect of waveguide curvature is shown in Fig. 8.

Conclusions

A microactuator was formed from combining a microtorsional transducer with an acoustic waveguide. Torsional vibration was transmitted along the waveguide, though flexural vibration was also generated with

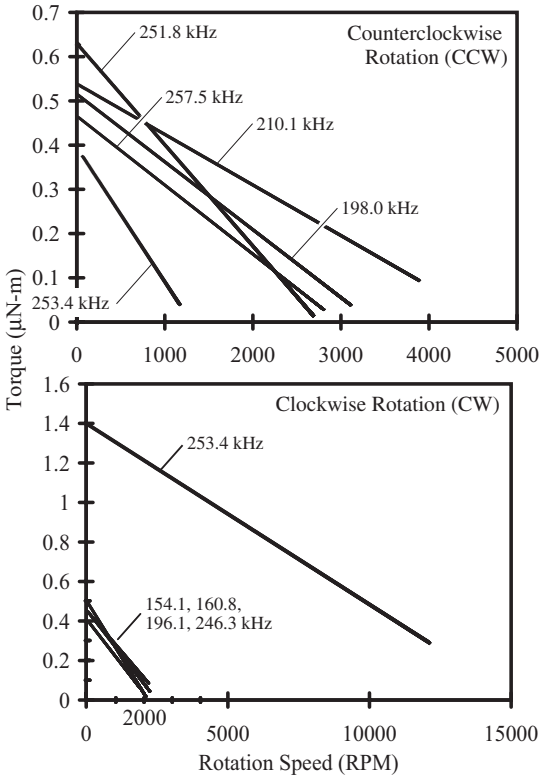

Figure 6: Torque versus speed for some of the resonance peaks in Fig. 5 using rotor α (*see* Fig. fig:device).

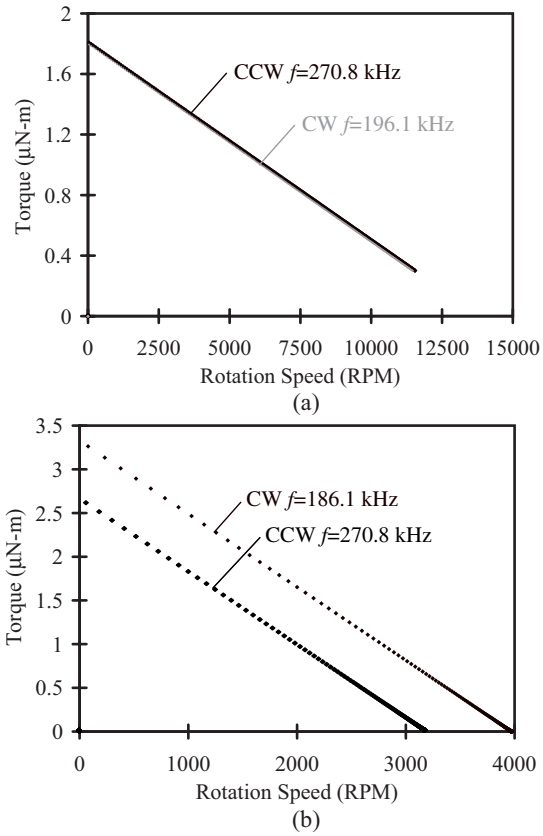

Figure 7: Torque versus speed for (a) rotor β and (b) rotor γ.

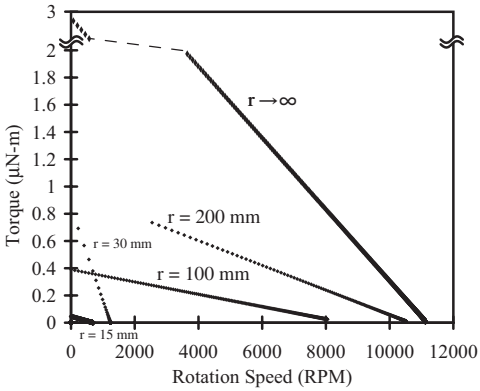

Figure 8: The effect of waveguide curvature on the rotation velocity of rotor α.

a great number of individual resonances due to the length of the waveguide. While a standing wave was present when the tip was free, a traveling wave developed upon the use of a rotor or damping material on the tip. Bidirectional rotation of a rotor was obtained at many of the waveguide resonances for a set of three different rotors, with 3 μN-m maximum torque and 11,500 rpm maximum rotation speed.

Acknowledgements

The authors wish to acknowledge a grant-in-aid from the Ministry of Education, Culture, Sports, Science and Technology for support of this work. The support of Taiheyo Cement is also gratefully acknowledged, and the authors wish to thank Suguru Wada, Osamu Ishiyama, and Teruya Sugihara of the Precision and Intelligence Laboratory's machine shop, whom machined the transducers used in this study.

References

[1] S. Ueha, T. Sugimoto, Y. Imaide, and M. Akiho, "A flexible ultrasonic lithotriptor," in Ultrasonics International 89 Conference Proceedings, 1989, pp. 1154–1158.

[2] R. Carotenuto, A. Iula, G. Caliano, and N. Lamberti, "Flexible piezoelectric motor based on an acoustic fiber," Applied Physics Letters, vol. 77, no. 12, 2000.

[3] J. Friend, K. Nakamura, and S. Ueha, "A novel torsional minitransducer using bulk pzt," in IEEE Ultrasonics Symposium, Munich, Germany, 2002.

[4] K. Nakamura, M. Kurosawa, H. Kurebayashi, and S. Ueha, "An estimation of load characteristics of an ultrasonic motor by measuring transient responses," IEEE Transactions on Ultrasonics, Ferroelectrics, and Frequency Control, vol. 38, no. 5, pp. 481–485, 1991.